Natural Frequencies and Vibration Modes of Laminated Composite Plates Reinforced with Arbitrary Curvilinear Fiber Shape Paths

Shinya HONDA[1] and Yoshihiro NARITA[2]

[1]*Corresponding author, Faculty of Engineering, Hokkaido University, N13W8, Kita-ku, Sapporo 060-8628, Hokkaido, Japan*

Email: honda@eng.hokudai.ac.jp, Tel/Fax: +81(11)706-6416

[2] *Faculty of Engineering, Hokkaido University,*

Email: ynarita@eng.hokudai.ac.jp

Abstract

The development of tow-placement technology has made it possible to control fiber tows individually and place fibers in curvilinear distinct paths in each layer of a laminated plate. This paper presents an analytical method for determining natural frequencies and vibration modes of laminated plates having such curvilinear reinforcing fibers. Spline functions are employed to represent arbitrarily shaped fibers, and Ritz solutions are used to derive frequency equations using series type shape functions. The strain energy is evaluated by numerical integration involving the fiber orientation angle, and is calculated using the derivative of the spline function in minute intervals. The results show that the natural frequencies obtained by the present method agree well with results from finite element analyses. The vibration mode shape contour plots of the plates are seen to reflect clear influences of the fiber shapes.

Keywords: laminated composite, curvilinear fibers, Spline function, natural frequency, vibration mode, Ritz method

1. Introduction

An innovative method was developed that allows the production of fiber reinforced composite materials with curved fibers by changing the direction of fiber-tows continuously. The automated tow-placement combines features of two conventional methods; the differential tow-payout capability of filament winding, and the compaction and cut-restart capabilities of automated tape laying. In the fiber placement process, individual prepreg tows are compacted by a heated rolling compaction device and laminated onto the lay-up surface [1].

The mechanical properties of the composite plates reinforced by curvilinear fibers depend strongly on the curvilinear shapes, and they possess non-uniform stiffness and anisotropy. Natural materials like bone also display local variations in properties and show better performance than homogenous materials [2]. Hence, compared with conventional plates with parallel fibers, there is a good potential that more effective fibrous composite plates designed using automated tow-placement equipment and curvilinear fibers are possible.

Some investigations of non-uniform local properties of fibrous composite plates have been reported. Martin and Leissa [3] presented a local property concept to improve the critical buckling loads of plates by an analysis which changes the fiber volume fraction locally in regions of plates using the Ritz method. Hyer and Lee [4] used the finite element analysis (FEA) method to analyze strength and buckling performance of plates with local properties including curvilinear fibers. They varied the fiber angles from one element to another, and it turned out that such plates have higher failure loads than plates with straight fibers. Recently, Gürdal [1， 5-7] and co-workers defined an arbitrary fiber shape by changing fiber orientation angles linearly between two different points, and confirmed by integrated research ranging over experimental and analytical methods that such plates had more desirable mechanical properties than conventional plates. The present authors [8] have calculated the natural frequencies of plates reinforced with quadratically shaped fibers using the Ritz method, and proved the advantage of plates with local property over the conventional parallel fiber plates in terms of design.

There are also publications about the optimization of plates with local properties. Setoodeh [9] and Abdalla [10] realized an optimum local property by distributing the lamination parameters in the plate optimally, and it was shown that plates with local properties were stiffer and had higher natural frequencies than plates with homogenous properties. However, they did not determine the optimum fiber shapes from the distributed parameters. Parnas [11] and co-workers presented a study of a weight minimizing problem of composite plates under stress constraints representing layer thickness and fiber shapes by bicubic Bezier surfaces and cubic Bezier curves, respectively.

Expecting to obtain similar effects with continuous curvilinear fibers, the present authors [12, 13] have studied the optimization problem of short fiber distributions in laminated fibrous composite plates in order to minimize the maximum deflection and to maximize the fundamental frequency of the plate. The optimum lamination parameter distributions obtained from Ref. [12] were calculated at each element in the finite element analysis (FEA) simultaneously using a gradient method, and the optimum short fiber distributions were thereby determined in each element by using the angle determination method from the lamination parameters which were proposed elsewhere [14, 15]. Further, combining a genetic algorithm [16] and a layerwise optimization concept [17, 18] solved the natural frequency maximization problem effectively [13]. The results showed that optimally distributed short fibers enabled the composite plate to give lower maximum static deflection and higher natural frequencies than conventional plates, and also indicated the specific orientations. Therefore, it was suggested that continuous curvilinear fibers would make it possible to reinforce fibrous composite plates more effectively than parallel fibers.

An effective analysis method is needed to reduce the exploration time to study the optimization problem of curvilinear fibers. The above reports analyze plate properties using the FEA. Indeed FEA is an efficient method but involves much calculation time. The present work proposes another effective method for analyzing vibrations of plates reinforced by arbitrarily shaped fibers. A spline function is employed to represent the arbitrarily shaped

fibers, and the frequency equations are derived using the Ritz method. In the present approach, the stiffnesses become functions of the position in the region of the plate since they are defined by the fiber orientation angles, and the strain energy stored in the plate is integrated numerically. The results from the present method show good agreement with the natural frequencies and mode shapes determined with general purpose FEA software, and the vibration modes resemble the fiber shapes clearly.

2. Method of Analysis

2-1. Bending stiffnesses of locally orthotropic plates

A symmetrically laminated, N-layered plate is considered here, as shown in Fig. 1. Distances from the plate middle surface to the upper surfaces of kth layer are z_k and rectangular plate dimensions are given by $a \times b \times h$ (thickness) in the O-xyz coordinate system. The h is small enough so that the plane stress state and the classical plate theory (CPT) are assumed here. The major and minor material principal axes are denoted by 1 and 2, respectively, and a fiber orientation angle θ is defined as the angle between the 1 direction and x axis. In the kth layer, stress-strain relationships in the directions of material principal axes are

$$\begin{Bmatrix} \sigma_1 \\ \sigma_2 \\ \tau_{12} \end{Bmatrix}^{(k)} = \begin{bmatrix} Q_{11} & Q_{12} & 0 \\ Q_{12} & Q_{22} & 0 \\ 0 & 0 & Q_{66} \end{bmatrix}^{(k)} \begin{Bmatrix} \varepsilon_1 \\ \varepsilon_2 \\ \gamma_{12} \end{Bmatrix} \tag{1}$$

where $Q_{11}^{(k)} = E_1/(1 - \nu_{12}\nu_{21})$, $Q_{22}^{(k)} = E_2/(1 - \nu_{12}\nu_{21})$, $Q_{12}^{(k)} = \nu_{12}E_2/(1 - \nu_{12}\nu_{21})$, $Q_{66}^{(k)} = G_{12}$. E_1 and E_2 are the moduli of elasticity in the 1 and 2 directions, G_{12} is the shear modulus, and ν_{12} and ν_{21} are the major and minor Poisson ratios. By rotating Eq. (1) in the amount of $\theta_k(x)$, which is the fiber orientation angle at the point p in kth layer, transformed stress-strain relations rotated with respect to the reference co-ordinate system O-xy shown in Fig. 1 are

$$\begin{Bmatrix} \sigma_x \\ \sigma_y \\ \tau_{xy} \end{Bmatrix}^{(k,x)} = \begin{bmatrix} \overline{Q}_{11} & \overline{Q}_{12} & \overline{Q}_{16} \\ \overline{Q}_{12} & \overline{Q}_{22} & \overline{Q}_{26} \\ \overline{Q}_{16} & \overline{Q}_{26} & \overline{Q}_{66} \end{bmatrix}^{(k,x)} \begin{Bmatrix} \varepsilon_x \\ \varepsilon_y \\ \gamma_{xy} \end{Bmatrix} \tag{2}$$

where $\overline{Q}_{ij}^{(k)}(x)$ are defined as functions of $\theta_k(x)$, and give different values at arbitrary points in each layer. The $\theta_k(x)$ values are constants for conventional laminated plates with parallel

fibers but they become functions with respect to the coordinate in the plate for the present locally orthotropic plate. The present analysis only accepts fibers expressed by the function of x and the material properties are homogenous along constant x in the y direction.

The relations of stress-strain and moment-curvature are obtained by the through-the-thickness integral of Eq. (2) which give stiffnesses

$$\begin{aligned} A_{ij}(x) &= \sum_{k=1}^{N} (z_k - z_{k-1}) \overline{Q_{ij}^k}(x) \\ B_{ij}(x) &= \frac{1}{2} \sum_{k=1}^{N} (z_k^2 - z_{k-1}^2) \overline{Q_{ij}^k}(x) \\ D_{ij}(x) &= \frac{1}{3} \sum_{k=1}^{N} (z_k^3 - z_{k-1}^3) \overline{Q_{ij}^k}(x) \end{aligned} \tag{3}$$

where z_k is the coordinate of the upper surface of the kth layer, and $A_{ij}(x)$, $B_{ij}(x)$ and $D_{ij}(x)$ (i, j = 1, 2, 6) are the local stretching, coupling and bending stiffnesses, respectively, and they are functions of the position in the region of the plate. When the plate is laminated symmetrically, the coupling stiffnesses $B_{ij}(x) = 0$; that is, the coupling between bending and extension vanishes. Then, only the bending stiffnesses are needed to analyze the transverse vibration properties of the laminated plate.

A fiber shape is defined as the function of x, and fiber orientation angles are given by the first derivative of the function to allow the plate stiffness to vary continuously. Therefore, not only a large number of degrees of freedom is necessary to represent arbitrarily shaped fibers, but also a relatively simple function is required for ease of treatment of integrals and derivatives. The spline function [19] satisfies these requirements simultaneously because it is a piecemeal polynomial function and is well suited to represent various shapes of curves.

The spline function of degree (m – 1) passing through n data points may be represented as a linear combination of B-spines, and defined by

$$s(x) = \sum_{i=1}^{n} \alpha_i B_{i,m}(x) \tag{4}$$

where α_i are coefficients of the linear combination, given by solving the equations $y_i = s(x_i)$ in

terms of known data points P_i (x_i, y_i) (i = 1, 2, ..., n.)

The B-spline of the (m – 1) degree is defined analytically by the divided difference and the truncated power function, but, using the de Boor-Cox recursion formula [19], the recurrence equation is defined as

$$B_{i,m}(x) = \frac{x - q_i}{q_{i+m-1} - q_i} B_{i,m-1}(x) + \frac{q_{i+m} - x}{q_{i+m} - q_{i+1}} B_{i+1,m-1}(x) \tag{5}$$

where q_i are nodes of P_i, and the B-spline of the (m – 1) degree $B_{i,m}(x)$ is composed of (m + 1) nodes. The $B_{i,m}(x)$ is a function with limited support and thus it is nonzero for $q_i < x < q_{i+m}$, and zero for $x \leq q_i$ and $x \geq q_{i+m}$.

When the coefficients α_i are known, the first derivative of Eq. (5) is expressed by

$$\frac{ds}{dx} = (m-1) \sum_{i=2}^{n} \frac{\alpha_i - \alpha_{i-1}}{q_{i+m-1} - q_i} B_{i,m-1}(x) \tag{6}$$

Then, the fiber orientation angle θ_k in the kth layer is given by

$$\theta_k(x) = \tan^{-1}\left(\frac{ds}{dx}\right) \tag{7}$$

The local bending stiffnesses due to curvilinear fibers are obtained by using Eqs. (2), (3) and (7).

2-2. Free Vibration Analysis

The Ritz method of analysis [20, 21], utilizing classical plate theory, is used for calculations of the natural frequency and vibration mode. In the present method, special forms of polynomials are employed as displacement functions [22]. They allow an analysis of the plate to include arbitrary combinations of typical boundary conditions (i. e., free, simply supported, and clamped edges.) The Ritz solutions require much smaller degrees of freedom in analysis than the FEA and have many advantages in handling other parameters, such as simple control parameters of the boundary conditions and the aspect ratios of rectangles. They require less computational effort than the FEA and this advantage is useful considering the application of the present method to optimization problems.

For small amplitude (linear) free vibration of a thin plate, the transverse displacement w may be written as

$$w(x,y,t) = W(x,y)\sin\omega t \tag{8}$$

where W is the amplitude and ω is an angular frequency. Then, the maximum strain energy due to the bending is expressed by

$$U_{\max} = \frac{1}{2}\iint_A \{\kappa\}^T [D]\{\kappa\}\, dA \tag{9}$$

where $[D]$ is the local stiffnesses given by Eq. (3), and $\{\kappa\}$ is a curvature vector defined by second derivatives written as

$$\{\kappa\} = \left\{ -\frac{\partial^2 w}{\partial x^2} \quad -\frac{\partial^2 w}{\partial y^2} \quad -2\frac{\partial^2 w}{\partial x \partial y} \right\}^T \tag{10}$$

The maximum kinetic energy is given by

$$T_{\max} = \frac{1}{2}\rho\omega^2 \iint_A W^2 dA \tag{11}$$

where ρ is the average mass per unit area. In the Ritz method, the amplitude is assumed to be the form of

$$W(\xi,\eta) = \sum_{m=0}^{M}\sum_{n=0}^{N} A_{mn} X_m(\xi)\, Y_n(\eta) \quad (m = 1,2,...,M; n = 1,2,...,N) \tag{12}$$

where A_{mn} is an unknown coefficient, M and N are the number of terms in the series expansion, and $X_m(\xi)$ and $Y_n(\eta)$ are the function modified so that all kinematical boundary conditions are satisfied at the edges with "boundary indices" [22].

$$\begin{aligned} X_m(\xi) &= \xi^m (\xi+1)^{B1} (\xi-1)^{B3} \\ Y_n(\eta) &= \eta^n (\eta+1)^{B2} (\eta-1)^{B4} \end{aligned} \tag{13}$$

where the $\xi = x/(a/2)$ and $\eta = y/(b/2)$ ($-1 \le \xi, \eta \le 1$) are non-dimensional coordinates along the x and y axes, and Bi (i = 1, 2, 3, 4) are the boundary indices, the order being defined in the clockwise direction from the left edge of the rectangle. The indices Bi = 0, 1, and 2 indicate free, simply supported and clamped edges, respectively. With the boundary indices Bi and Eqs. (13), the Ritz method can accommodate arbitrary sets of the edge conditions.

After substituting Eq. (12) into Eqs. (9) - (11), we obtain the stationary value by

$$\frac{\partial(T_{\max} - U_{\max})}{\partial A_{mn}} = 0 \tag{14}$$

This minimizing process gives a set of linear simultaneous equations in terms of the coefficient A_{mn}. The eigenvalues Ω are extracted using Cholesky reduction followed by Householder diagonalization. Since the present shape function is defined by a series expansion, the differences between adjacent lows or columns in the resulting matrix for the frequency equation are becoming small as the numbers of terms M and N in Eq. (12) increase. This causes a non-positive defined matrix in the process of extracting eigenvalues, and referring [22], $M = N = 10$ is taken in this study. The eigenvalue Ω is a frequency parameter defined as

$$\Omega = \omega a^2 \sqrt{\frac{\rho}{D_0}} \tag{15}$$

where $D_0 = E_2 h^3/12(1 - \nu_{12}\nu_{21})$ is a reference bending stiffness. Further, the vibration mode is determined by calculating relative differences in A_{mn} after substituting Ω into the linear simultaneous equations obtained by Eq. (14). It is difficult to integrate Eq. (9) analytically and a numerical integration is employed where the trapezoid formula [23] is applied due to its simplicity and ease for local properties. In the integration process, orthotropic properties are assumed in the minute intervals, and the fiber orientation angles defined in Eq. (7) are applied to each interval. If the number of intervals is large enough, the fibers may be regarded as continuous fibers.

3. Numerical Results

Calculation procedures for the present results are as follows.

Spline function

Three degrees of spline and five data points P_i (ξ_i, η_i) (i = 1, 2, ..., 5) which define the shape of fibers in the O-$\xi\eta$ co-ordinates are used in the present paper. For example, in the quasi-cosine shaped fibers shown in Fig. 2, the data points are P_1 (-1, -0.5), P_2 (-0.5, 0), P_3 (0, 0.5), P_4 (0.5, 0), and P_5 (1, -0.5). For square plates (a/b = 1), the fiber shapes in the O-$\xi\eta$

coordinates are similar to those in the *O-xy* co-ordinates, and they are extended or compressed for rectangular plates. The number of divisions between data points of the spline is 25, and thus the plate is divided into 25 × 4 = 100 thin rectangles in the x or ξ direction, where the spline is the function of x, and similar functions are assumed in the y direction. These dividing points are used as integral points in the numerical integration.

Fiber shapes

Figure 3 illustrates square plates with three kinds of reinforcing fiber shapes which are (i) quasi-quadratic, (ii) quasi-cubic, and (iii) arbitrary. Each data point indicated in the left column in Fig. 3 is listed in Table 1 and these layers are defined as "+ layer". The symmetric shape with respect to each axis is defined as "- layer" and shown in the middle column in Fig. 4. The right column in Fig. 4 shows the overlapping views.

Boundary conditions and layup configurations

The material is assumed as graphite / epoxy (CFRP) with E_1 = 138 GPa, E_2 = 8.96 GPa, G_{12} = 7.1 GPa, and v_{12} = 0.30 for all results. The layup configuration, boundary condition, fiber shape and aspect ratio for each section are listed in Table 2. When the layup is “single” the plate has a “+ layer” fiber shape indicated in the “fiber shape” column in Table 2. For layered plates, The [*/*/…/*]s describes the lay-up configuration, where the leftmost symbol * is the outermost layer and subscript “s” means symmetry. Except for section 3-4, a plate is composed of symmetric layers with “+ layer” and “-layer”, and stacking sequences are listed in Table 2. The boundary conditions of the plates are identified by the four capital abbreviations with F, S, and C denoting the free, simply supported and clamped edges, arranged in counterclockwise order starting from the plate left edge. For example, the totally clamped plate is expressed by CCCC and the cantilever plate with clamped left edge is CFFF.

3-1. Numerical integration and convergence study

The present study employs the trapezoid formula to calculate strain energy in Eq. (9). A convergence test on the integration rule is presented in Table 3 for the different numbers of divisions. The lowest four frequencies are calculated for the single-layer square plate

reinforced by the quadratically shaped fibers (Fig. 3(i)). The frequencies monotonically decrease as the number of divisions increases, and they converge to four significant digits when the number of divisions is 5000. The difference for each frequency is less than 1 % between divisions 5000 and 100, and thus the present study employs 100 divisions to calculate frequencies and mode shapes.

3-2.Comparison with results from finite element analysis

A comparison of the present results and those from FEA was made to assess the accuracy of the present method. Figure 4 shows the variations of the lowest four frequency parameters Ω, calculated by the present Ritz method and the FEA, for the plate reinforced by quasi-cosine shaped fibers, approximated by $y = 0.5\times A\times\cos\{\pi x\}$, when the coefficient A is varied from 0.1 to 10 (for Fig. 2, $A = 1$). The results are shown for totally clamped (CCCC) single layer square ($a/b = 1$) plates. The vertical axis shows the frequency parameters Ω, and the horizontal axis shows the coefficient A in logarithmic scale. The general purpose commercial FEA software (ANSYS) is employed for the comparison. The plate is divided into 20 × 20 elements and the number of divisions in the horizontal direction is 20. A straight fiber is assumed at each element but different fiber orientation angles varying continuously between adjacent elements are defined by orienting the element coordinate using ANSYS user subroutines (USERAN and USANLY). The comparison of the present method with the FEA in Fig. 4 shows that the frequency parameters from both methods result in similar variations although the FEA results have globally lower frequency values than the present ones. The present Ritz method give upper bounds of solutions because the displacement functions satisfy only kinematical boundary conditions. In contrast, the FEA results do not guarantee either upper or lower bounds. Therefore, the results confirm the validity of the present method.

The advantage of the present method is the lower calculation time than the FEA. The average CPU times (Intel Core2 CPU 6600@ 2.40 GHz, 2.40 GHz) for the present Ritz method and the FEA batch run are 3.997 and 4.860 [sec], respectively, where the plate is the totally clamped single-layer square plate. The clamped boundary is advantageous for the FEA

since the size of global matrix for eigen value calculation becomes small. On the other hand, it is disadvantageous for the present Ritz method since the orders of shape functions Eqs. (13) become large. Even the disadvantageous boundary condition, the present Ritz method has about one second faster calculation time than FEA. In the case of applying the present method to the optimization problem which requires a vast number of reputations of the calculation, the present method is advantageous.

3-3. Frequency and vibration mode for laminated plates

Figures 5-7 show the lowest four frequency parameters and vibration modes for cases (i)-(iii) (Fig. 3), respectively. The mark "×" indicates the maximum amplitude point. The thick lines represent the nodal lines (i.e., lines of zero displacement), and thin lines denote the displacement contour lines, where the interval between the nodal line and the maximum amplitude point is divided into ten equal increments. The results are for (a) a single-layer plate composed of only "+ layer", and (b) the symmetrically 4-layered [+/-]s, (c) 6-layered [+/-/-]s and (d) 8-layered [+/-/-/-]s laminated plates. All plates are totally simply supported. The thickness is constant for all the plates, and thus the number of layers suggests the thickness proportion of the "+ layer" to "- layer".

It is verified from Figs. 5-7 that each vibration mode is clearly affected by the curvilinear shapes of the fibers. For the single-layer plate in Fig. 5 (a), the mode shapes resembling the quadratically shaped fibers are given in the first and third modes, and the nodal lines which are similar to the fiber shape appear in the second and the fourth modes. This result agrees well with that of the literature [8]. In Fig. 5 (b), half of the thickness is composed of the "- layer", but the vibration modes are strongly affected by the "+ layer". This result is in accord with the physical fact that in the laminated plate the outer layer has a stronger influence on the plate vibration than the inner layer, since the bending stiffnesses are defined by the differences of the cubic of distance from plate mid-surface z_k in Eq. (3). The influence of the "+ layer" is diminishing gradually as the "- layer" thickens in Fig. 5 (c) and (d). It is remarkable that the quadratically shaped nodal lines in the second and the fourth modes are becoming straight. The mode shapes and frequencies from the FEA, calculated by the same method with Section

3.1, are shown in Fig. 8 for the plate with (i) quadratically shaped fibers. The results agree well with the present results in Fig. 5.

In Fig. 6, mode shapes are similarly affected by the fiber shapes in the first mode, and nodal lines which are similar to the fiber shape are seen for the second and third modes. As the "- layer" becomes thick, the skewness is diminishing from the first mode, and the nodal lines are becoming straight for the second and third modes. There is no clear change for the fourth mode compared with other three modes although the mode shape is approaching a "2 : 2" mode as the "- layer" becomes thicker. The half waves are denoted as "m : n" in the "x : y" directions, respectively. The phenomena in Fig. 5 and 6 are also found in Fig. 7. The third and fourth modes are "1 : 3" and "2 : 1" in Fig. 7(a), (b), respectively, and the order is reversed in Fig. 7 (d). Further, through Figs. 5-7, the frequency parameters become higher as the "- layer" becomes thicker.

Based on the above discussion, it is concluded that a plate with curvilinearly reinforcing fibers resembles the fiber shape in its mode shapes and has different modes from conventional composite plates with parallel fibers. The influence of the fiber shape is diminished gradually as symmetric layers are inserted into the inner layer. For the frequency parameters, the plate with thin outer "+ layer" and thick inner "- layer" gives higher values. This results agree with those from the literature [18], that the optimum layup configuration which gives the maximum fundamental frequency of conventional plates with symmetric 8-layers for the totally simply supported square plate is [45/-45/-45/-45]s which is composed of a thin outer layer of 45° and a thick symmetric inner layer of -45°.

The present three kinds of plates with curvilinear fibers give lower fundamental frequencies than the parallel fiber plate [45/-45/-45/-45]s whose fundamental frequency is 56.32. Frequencies are strongly affected by the boundary conditions and it is known that ±45° fiber orientation angles are shapes suitable to the simply supported edge [13]. The present plates with (i) quasi-quadratic and (iii) arbitrary fibers have ±45° fiber shapes adjacent to the left and right edges. This is because both plates result in higher fundamental frequencies than

the plate with (iii) quasi-cubic fibers. Although the present shapes give lower fundamental frequencies than that with parallel fibers, the appropriate curvilinear fibers may adapt to complex boundary conditions more flexibly than the parallel fibers, resulting in higher fundamental frequencies.

3-4. Overlapping of different shapes

Figure 9 illustrates an overlapping view of the three kinds of "+ layers" which are indicated in Fig. 4. The plate is square and symmetrically 6-layered. Its layup configuration is [+(i)/+(ii)/+(iii)]s. The lowest four vibration modes and frequency parameters are given in Fig. 10 when the plate is totally simply supported. In the first mode, the mode shape is strongly affected by the (i) quadratically shaped fibers similar to the first mode of Fig. 5 (a). However, the mode shape is slightly skewed and asymmetric due to the influence of the inner layers. For the other modes, the influence of the inner layer is stronger than it is for the first mode although a clear effect of the outermost layer is still remaining.

3-5. Effect of boundary conditions

Figure 11 shows the non-dimensional frequency parameters Ω and vibration modes of the square plate with (iii) arbitrary shaped fibers for (a) CFFF (cantilever), (b) SCFF, and (c) CCSF boundary conditions. The number of layers is symmetrically 4-layered [+/-]s since the influence of the "+ layer" clearly appears in the vibration mode.

The nodal line in the second mode of Fig. 11 (a) resembles the fiber shape of the "+ layer" and it occurs in the upper half region of the plate. Since the nodal line of the isotropic plate appears in the middle of the plate, this difference between the plates is caused by the fiber shapes. The same comments may be made for other boundary conditions.

3-6. Effect of aspect ratio

Figure 12 shows the results for rectangular plates with three kinds of fiber shapes. The aspect ratio is 1.5 (a/b = 1.5). The plate is totally simply supported and the layup configuration is symmetrically 4-layered [+/-]s.

It is evident from Fig. 12 that the nodal lines are significantly affected by the curvilinear fiber shapes even when the plate is not square. Furthermore, due to the aspect ratio, the second and third modes for (i) and the third and fourth modes for (ii) and (iii) are replaced when compared with Figs. 5-7 (b). These phenomena are also confirmed for isotropic plates.

4. Conclusion

The natural frequencies and vibration modes were calculated for laminated composite plates with curvilinearly reinforcing fibers which are represented by spline function using the Ritz method.

The present results were compared with those of finite element analysis (FEA), and the two agreed well. The present method showed that plates with curvilinear fibers resembled the fiber shapes clearly in the vibration mode shapes and gave specific mode shapes which would not result from conventional plates with parallel fibers. The effect of the fiber shapes were diminished by inserting symmetric layers toward the outermost layer into the inner layers. Plates with thin outer layers and thick inner layers which are symmetric to the outer layer gave higher frequencies than those with thick outermost layers. Further, a plate having laminated layers with different fiber shapes resulted in complex mode shapes. From the study for various boundary conditions, it was found that the mode shapes were affected by both boundary conditions and the curvilinear fibers. For rectangular plates, the curvilinear fibers influenced the mode shapes, and mode replacement was confirmed when they are compared with the results for square plates.

Acknowledgement

This work was supported by KAKENHI (22760164), and the authors would like to express our gratitude to Prof. A. W. Leissa, a professor emeritus at Ohio State University, for his constructive comments.

References

1 C. S. Lopes, Z. Gürdal, P. P. Camanho, Variable-stiffness composite panels: buckling and first-ply failure improvements over straight-fibre laminates, *Computers & Structures* 86 (2008) 897-907.

2 B. Giri, S. Tadano, K. Fujisaki, M. Todoh, Microstructure of bone around natural hole in bovine lumber vertebra, *Journal of Biomechanical Science and Engineering* 2 (2007) 1-11.

3 A. F. Martin, A. W. Leissa, Application of the Ritz method to plane elasticity problems for composite sheets with variable fiber spacing, *International Journal of Numerical Methods in Engineering* 28 (1989) 1813-1825

4 M. H. Hyer, H. H. Lee, The use of curvilinear fiber format to improve buckling resistance of composite plates with central circular holes, *Composite Structures* 18 (1991) 239-261.

5 Z. Gürdal, R. Olmedo, In-plane response of laminates with spatially varying fiber orientation: variable stiffness concept, *AIAA Journal* 31 (1993) 751-758.

6 Z. Güdal Z, B. F. Tatting, C. K. Wu, Variable stiffness composite panels: effects of stiffness variation on the in-plane and buckling response, *Composites Part A*, 39, (2008) 911-922.

7 C. S. Lopes, P. P. Camanho, Z. Güdal, B. F. Tatting, Progressive failure analysis of tow-placed, variable-stiffness panels, *Solids and Structures* 44 (2007) 8493-8516.

8 S. Honda, Y. Oonishi, Y. Narita, K. Sasaki, Vibration analysis of composite rectangular plates reinforced along curved lines, *Journal of System, Design and Dynamics* 2 (2008) 76-82.

9 S. Setoodeh, M. M. Abdalla, Z. Gürdal, Design of variable–stiffness laminates using lamination parameters, *Composites Part B: Engineering* 37 (2006) 301-309.

10 M. M. Abdalla, S. Setoodeh, Z. Gürdal, Design of variable stiffness composite panels for maximum fundamental frequency using lamination parameters, *Composite structures* 81(2007) 283-291.

11 L. Parnas, S. Oral, Ü. Ceyhan, Optimum design of composite structures with curved fiber courses, *Composites Science and Technology* 63 (2003) 1071-1082.

12 S. Honda, Y. Narita, Design of composite plates with optimally distributed short fibers, *Proceeding of Sixteenth International Conference on Composite Materials* CD-ROM (MoKA1-03), Kyoto, July 2007.

13 S. Honda, Y. Narita, Design for the maximum natural frequency of laminated composite plates by optimally distributed short fibers, *Journal of System Design and Dynamics* 2 (2009) 1195-1205.

14 S. Honda, Y. Narita, K. Sasaki, Discrete optimization for vibration design of composite plates by using lamination parameters, *Advanced Composite Materials* 18 (2009) 297-314.

15 S. Honda, Y. Narita, K. Sasaki, Optimization for the maximum buckling loads of laminated composite plates -- comparison of various design method, *Key Engineering Materials*, 334-335 (2007) 89- 92.

16 L. R. Riche, R. T. Haftka., Optimization of laminate stacking sequence for buckling load maximization by genetic algorithm, *AIAA Journal* 31 (1993) 951-

956.
17 Y. Narita, G. J. Turvey, Maximizing the buckling loads of symmetrically laminated composite rectangular plates using a layerwise optimization approach, *Journal Mechanical Engineering Science* 218 (2004) 681-691.
18 Y. Narita, Layerwise optimization for the maximum fundamental frequency of laminated composite plates, *Journal of Sound and Vibration* 263 (2003)1005-1016.
19 C. Boor, *A practical guide to splines*, Splinger, New York, 2001
20 A. W. Leissa, The historical bases of the Rayleigh and Ritz methods, *Journal of Sound and Vibration* 217 (1998) 927-944
21 Y. Narita, A. W. Leissa, Frequency and mode shapes of cantilevered laminated composite plates, *Journal of Sound and Vibration* 154 (1992) 161-172
22 Y. Narita, Combinations for the free-vibration behaviors of anisotropic rectangular plates under general edge condition, *Journal of Applied Mechanics* 67 (2000) 568-573
23 W. H. Press, S. A. Teukolsky, W. T. Vetterling, B. P. Flannery, *Numerical Recipes in Fortran 77*, Cambridge University Press, London, 1992

Figure captions:

Fig. 1 The coordinate system for the symmetrically laminated plate

Fig. 2 Example of data points for quasi-cosine shaped fibers (a/b = 1)

Fig. 3 Plates with (i) quadratically, (ii) cubically, and (iii) arbitrarily shaped fibers (a/b = 1)

Fig. 4 Comparison between the Ritz results and those from the FEA for totally clamped square plates with quasi-cosine shaped fibers (a/b = 1)

Fig. 5 The lowest four frequency parameters Ω and vibration modes of plates with (i) quadratically shaped fibers and totally simply supported edges (a/b = 1)

Fig. 6 The lowest four frequency parameters Ω and vibration modes of plates with (ii) cubically shaped fibers and totally simply supported edges (a/b = 1)

Fig. 7 The lowest four frequency parameters Ω and vibration modes of plates with (iii) arbitrary shaped fibers and totally simply supported edges (a/b = 1)

Fig. 8 The lowest four frequency parameters Ω and vibration modes of plates with (i) quadratically shaped fibers and totally simply supported edges (a/b = 1) calculated by FEA

Fig. 9 The plate laminated layers with three kinds of fiber shapes [(i)/(ii)/(iii)]s (a/b = 1)

Fig. 10 The lowest four frequency parameters Ω and vibration modes of the totally simply supported square plate of laminated layers with three kinds of fiber shapes [(i)/(ii)/(iii)]s (a/b = 1)

Fig. 11 The lowest four frequency parameters Ω and vibration modes of symmetrically 4-layered plates with (iii) arbitrarily shaped fibers and various boundary conditions (a/b = 1)

Fig. 12 The lowest four frequency parameters Ω and vibration modes of symmetrically 4-layered plates with (i) quadratically, (ii) cubically, and (iii) arbitrarily shaped fibers and totally simply supported edges (a/b = 1.5)

Tables captions:

Table 1 Data points for each layer with curvilinearly shaped fibers

Table 2 Layup configuration, boundary condition, fiber shape, and aspect ratio for each result indicated in each Section of Capter 3.

Table 3 Convergence of the first four frequencies Ω on the integration rule for the single-layer plate with quadratically shaped fibers (a/b = 1)

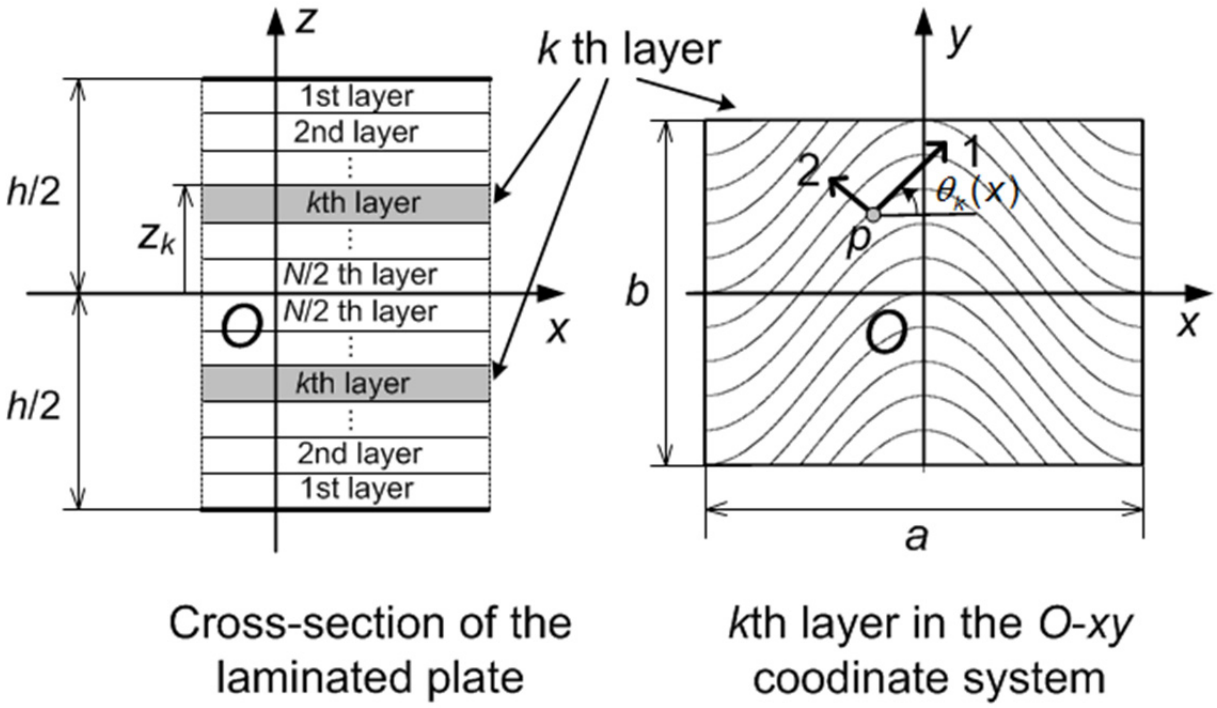

Fig. 1 The co-ordinate systems for the present symmetrically lamianted plate

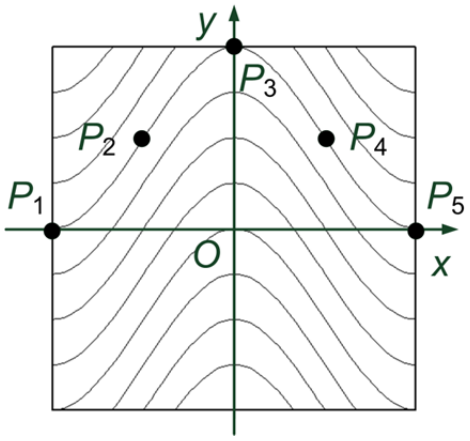

Fig. 2 Example of data points for quadratically shaped fibers ($a/b = 1$)

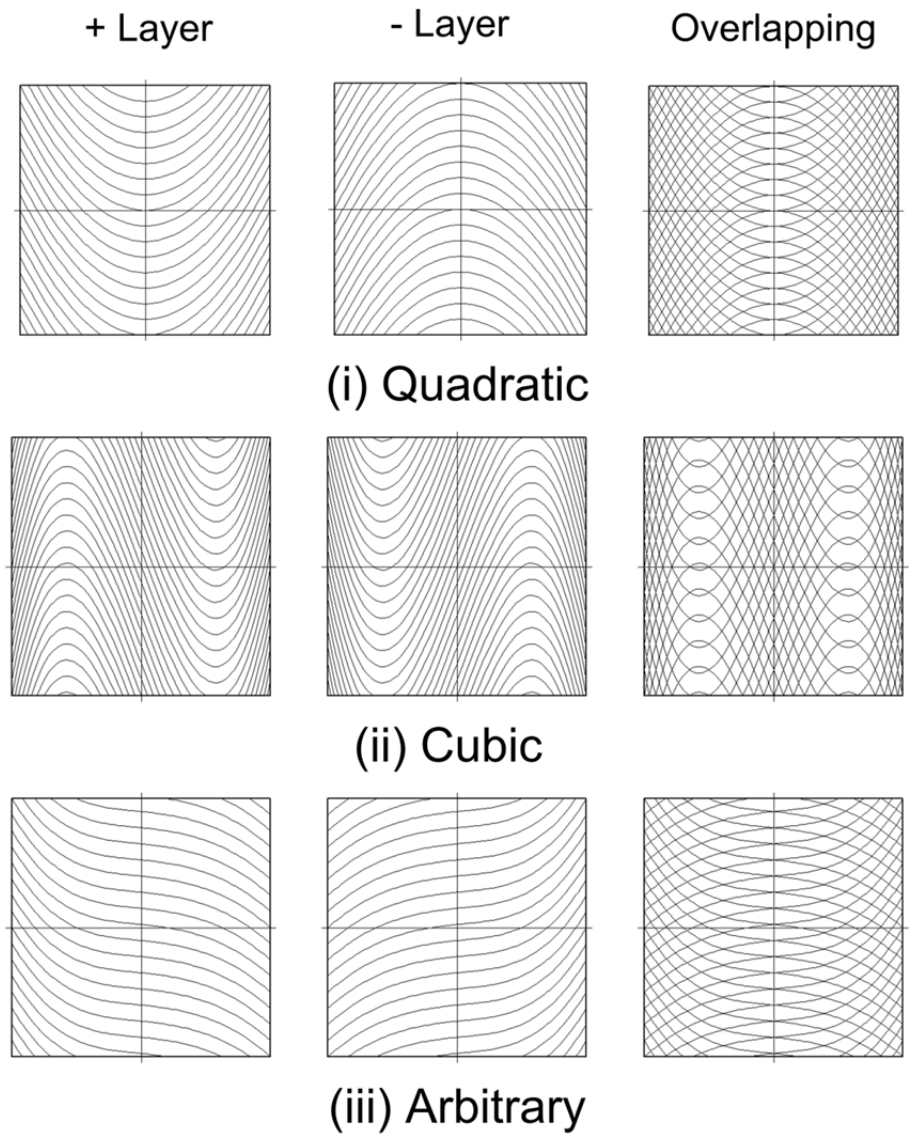

Fig. 3 Plates with (i) quadratically, (ii) cubically, and (iii) arbitrarily shaped fibers ($a/b = 1$)

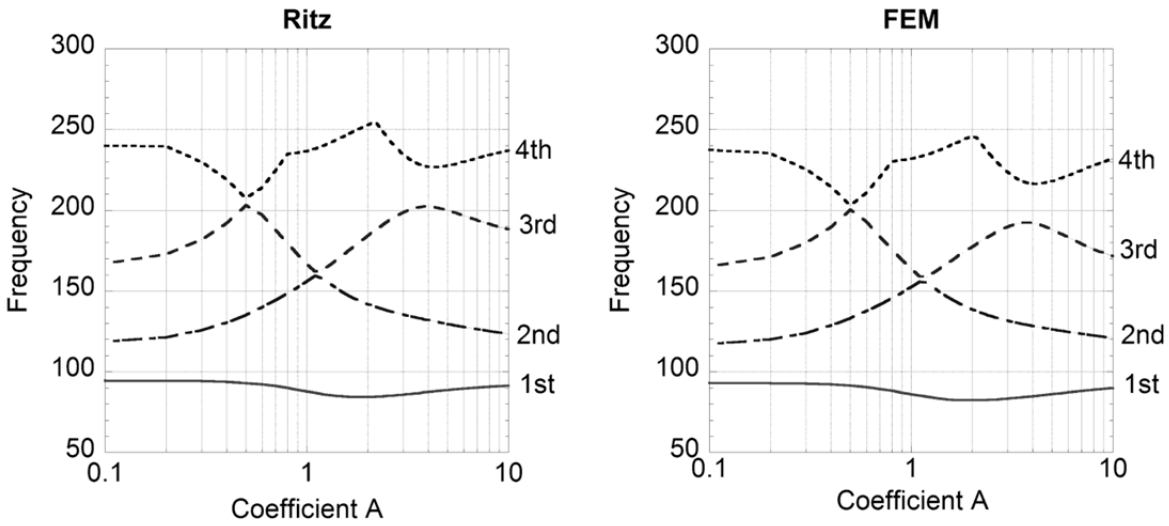

Fig. 4 Comparison between the Ritz results and those from the FEA for totally clamped square plates with quasi-cosine shaped fibers ($a/b = 1$)

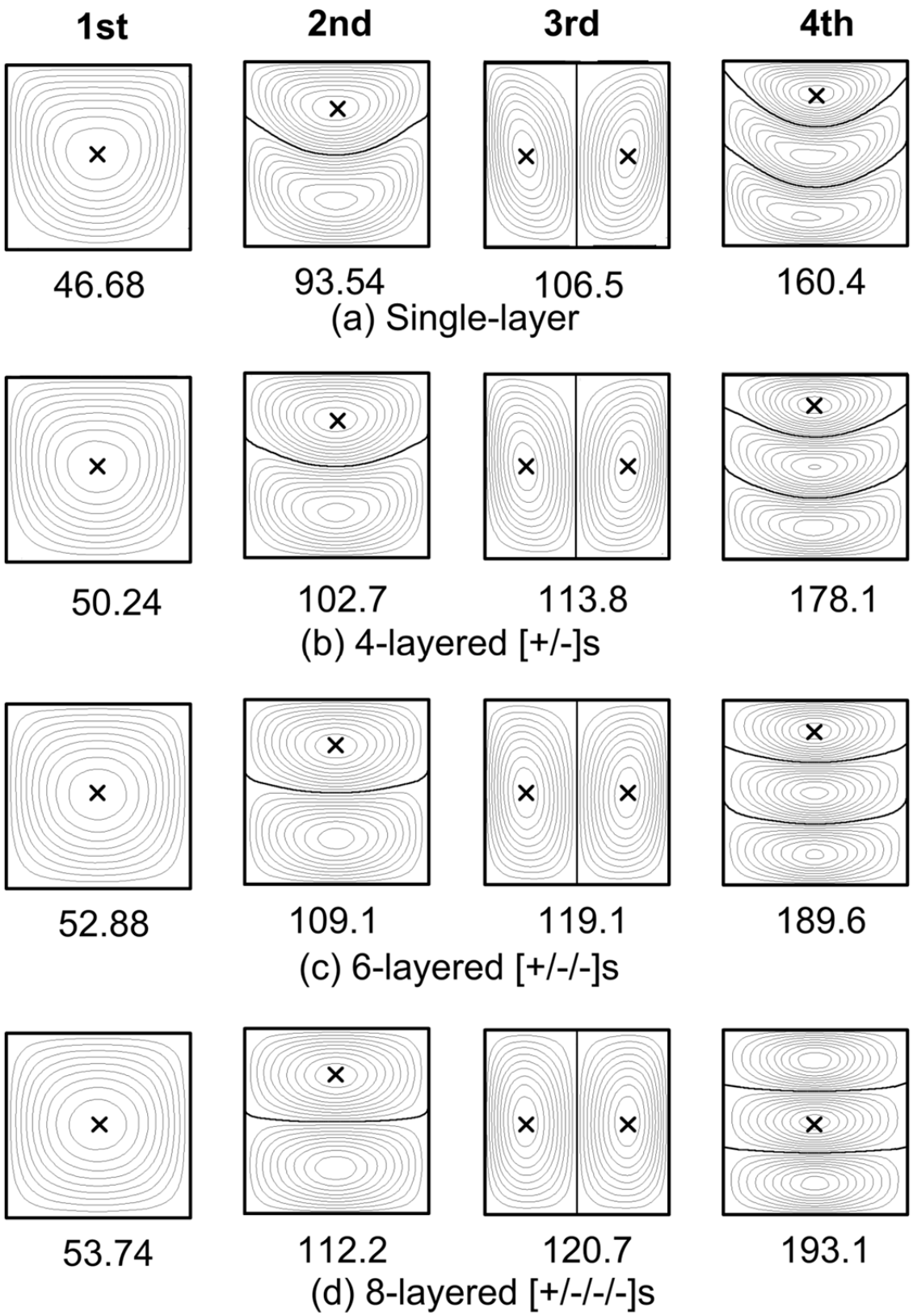

Fig. 5 The lowest four frequency parameters and vibration modes of plates with (i) quadratically shaped fibers and totally simply supported edges ($a/b = 1$)

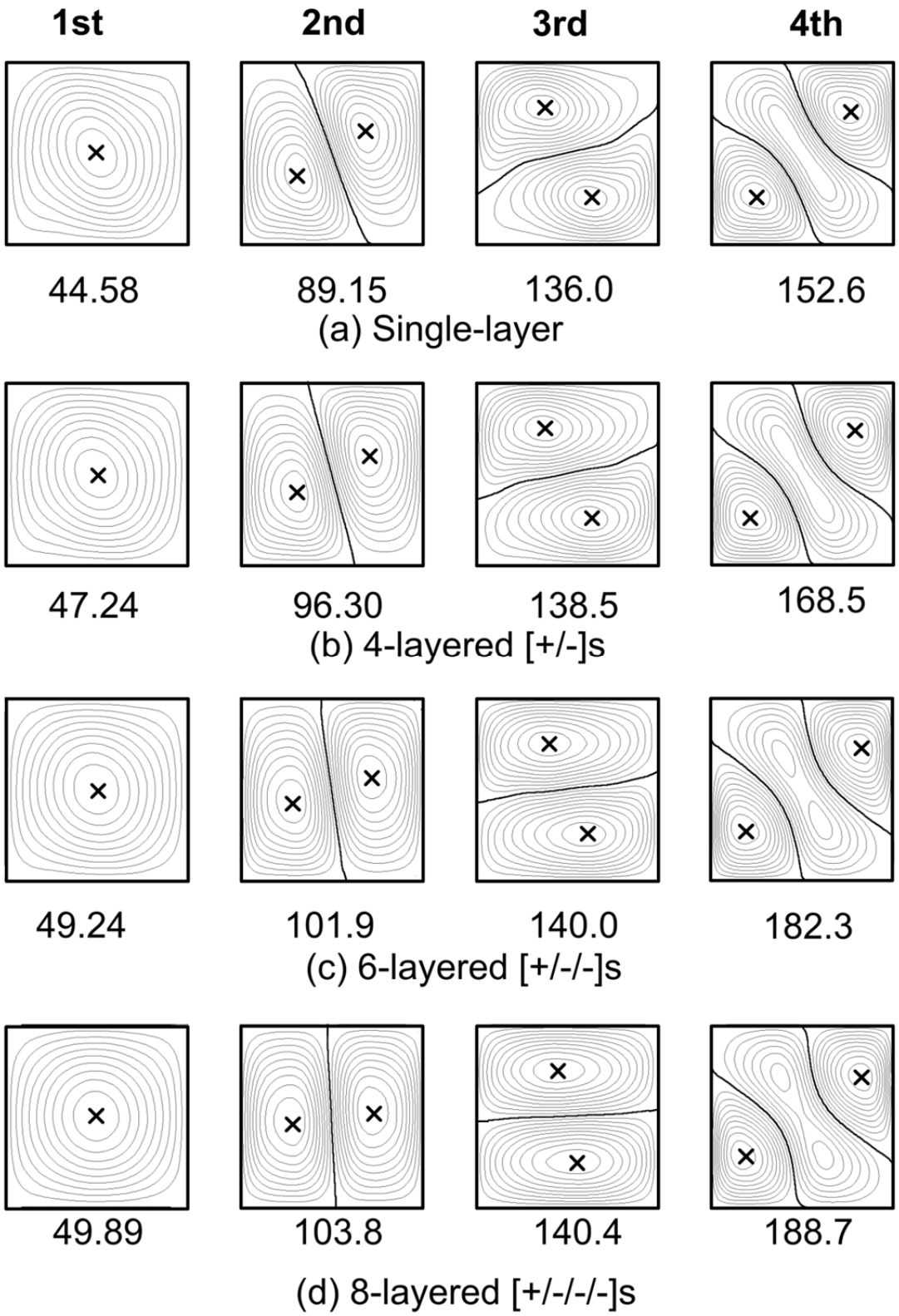

Fig. 6 The lowest four frequency parameters and vibration modes of plates with (ii) cubically shaped fibers and totally simply supported edges ($a/b = 1$)

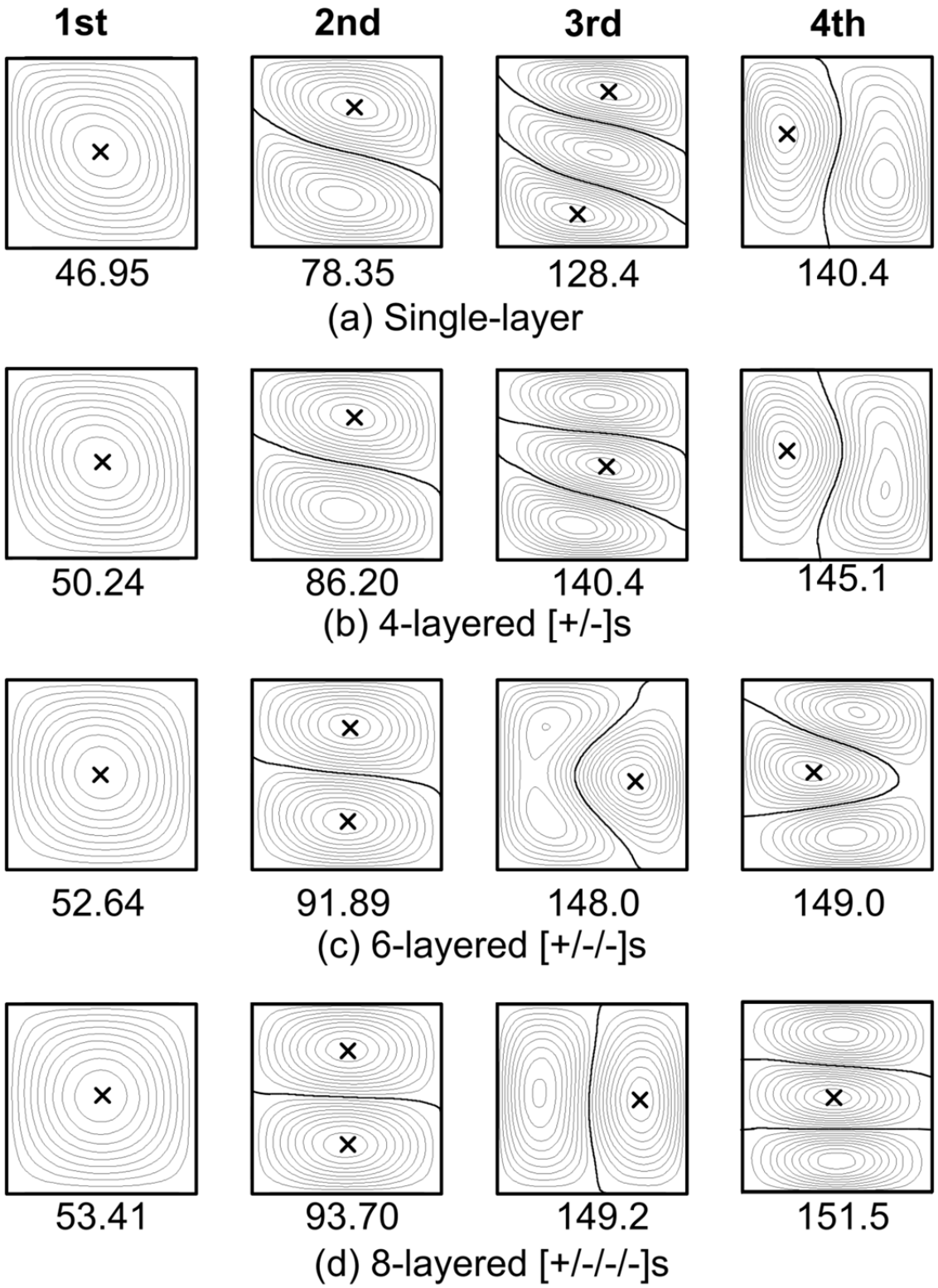

Fig. 7 The lowest four frequency parameters and vibration modes of plates with (iii) arbitrary shaped fibers and totally simply supported edges ($a/b = 1$)

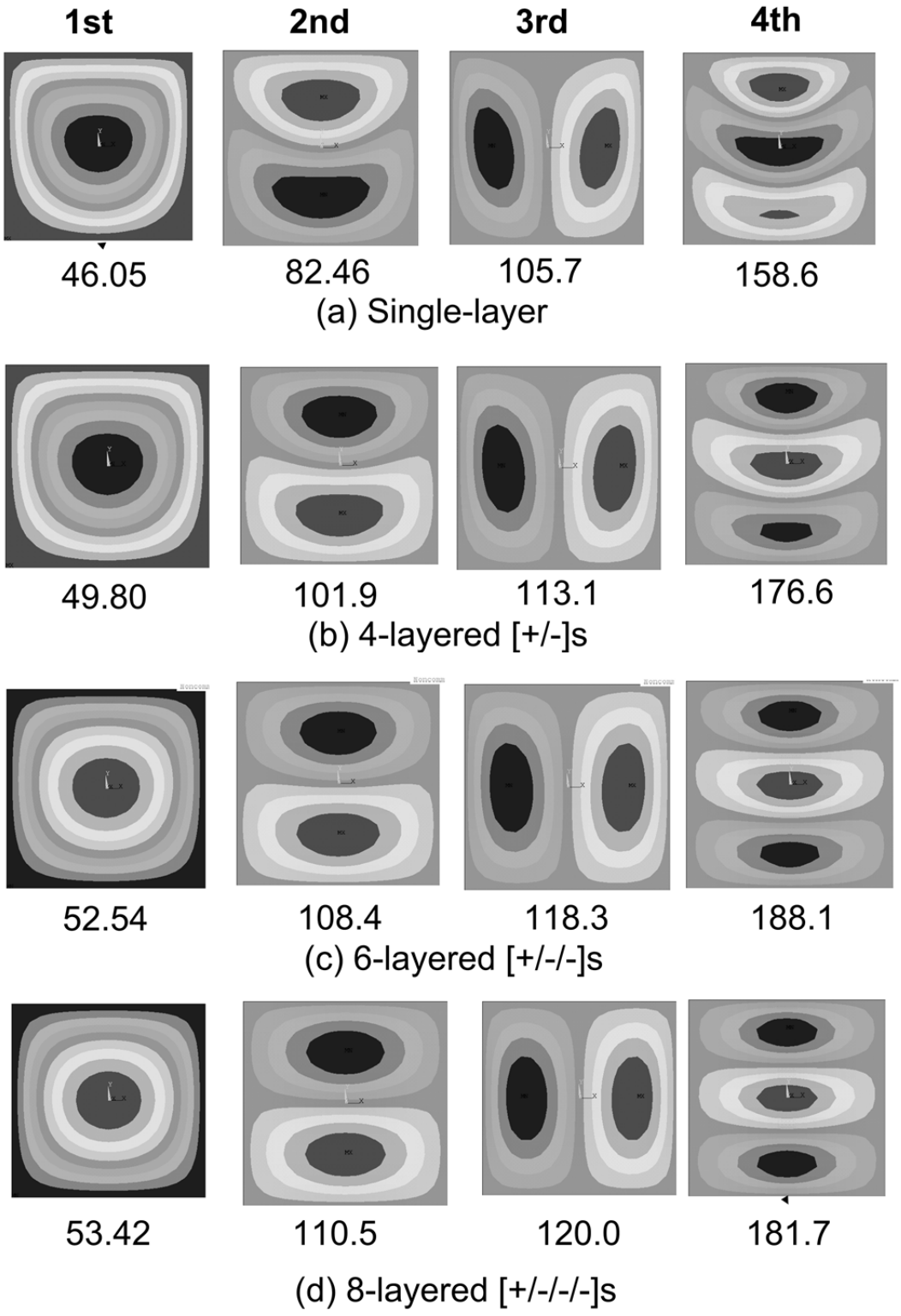

Fig. 8 The lowest four frequency parameters and vibration modes of plates with (i) quadratically shaped fibers and totally simply supported edges (a/b = 1) calculated by FEA

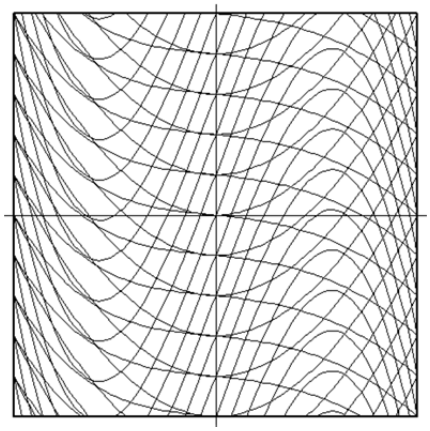

Fig. 9 The plate laminated layers with three kinds of fiber shapes [(i)/(ii)/(iii)]s (a/b = 1)

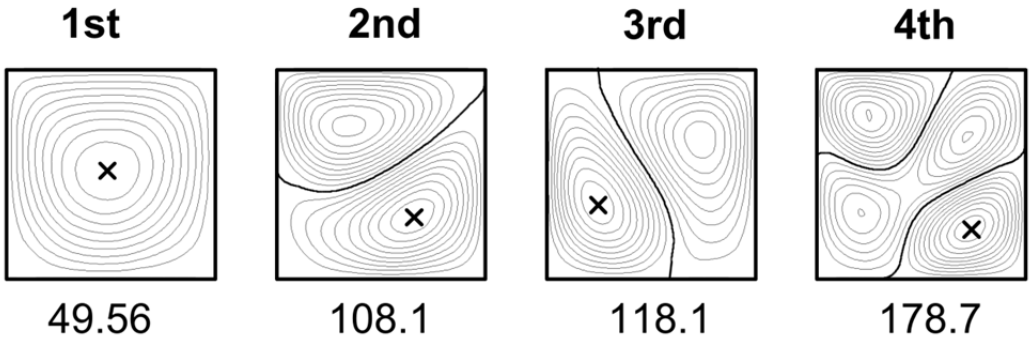

Fig. 10 The lowest four frequency parameters and vibration modes of the totally simply supported square plate of laminated layers with three kinds of fiber shapes [(i)/(ii)/(iii)]s (a/b = 1)

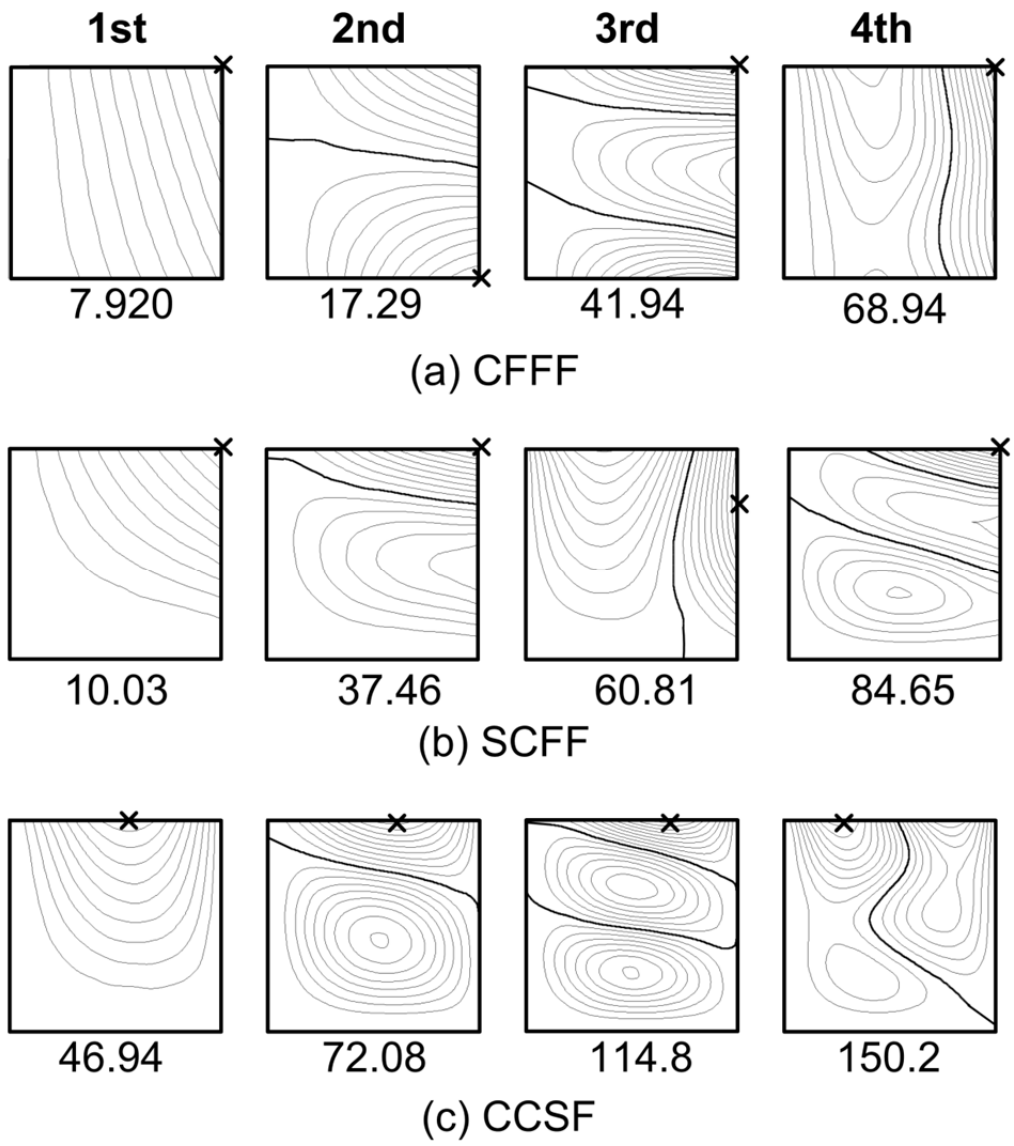

Fig. 11 The lowest four frequency parameters and vibration modes of symmetrically 4-layered plates with (iii) arbitrarily shaped fibers and various boundary conditions (a/b = 1)

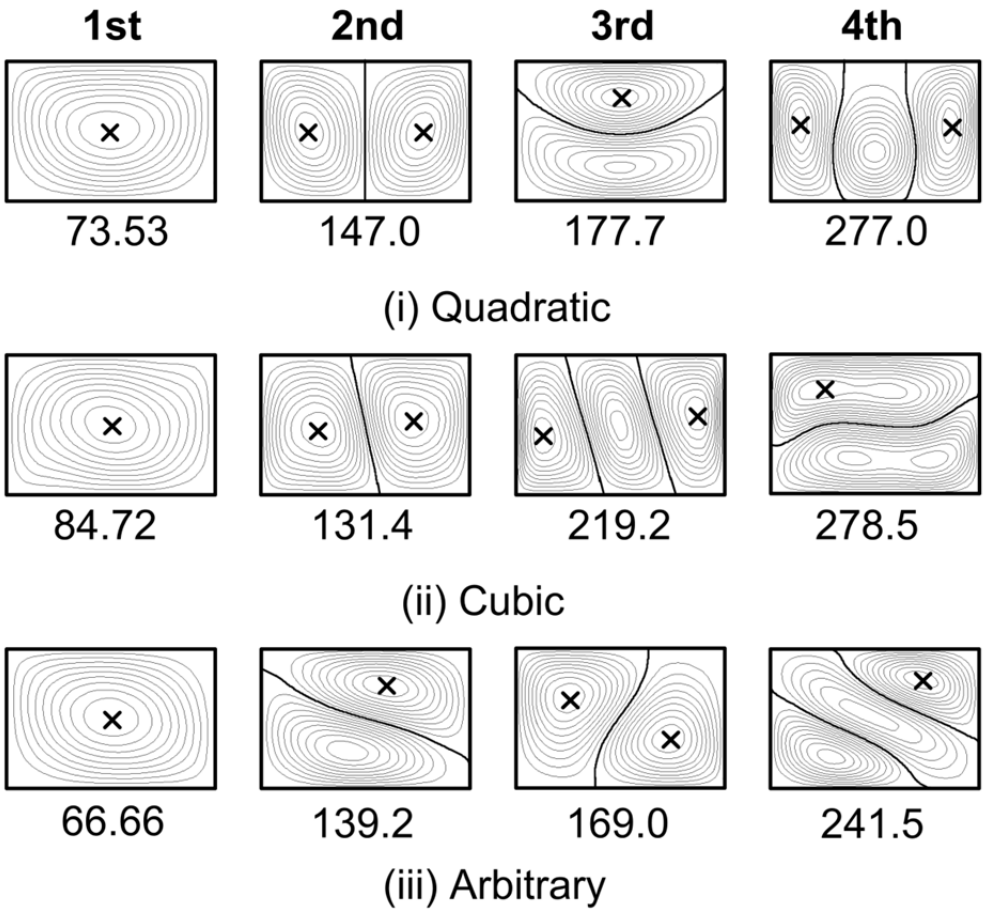

Fig. 12 The lowest four frequency parameters and vibration modes of symmetrically 4-layered plates with (i) quadratically, (ii) cubically, and (iii) arbitrarily shaped fibers and totally simply supported edges (*a*/b = 1.5)

Table 1. Data points for each layer with curvilinearly shaped fibers

		x				
		-1	-0.5	0	0.5	1
y	(i) Quadratic	1	0.25	0	0.25	1
	(ii) Cubic	0	1	0	-1	0
	(iii) arbitrary	1	0.5	0.4	0.3	0

Table 2. Lay-up configuration, boundary condition, fiber shape, and aspect ratio for each result indicated in each Section of Capter 3..

Section	Lay-up	B. C.	Fiber shape	Aspect ratio (= *a*/*b*)
3-1	single	SSSS	(i) quadratic	1
3-2	single	CCCC	cosine (Fig. 2)	1
3-3	single 4-layered [+/-]s 6-layered [+/-/-]s 8-layered [+/-/-/-]s	SSSS	(i) quadratic (ii) cubic (iii) arbitrary	1
3-4	6-layered [+(i)/+(ii)/+(iii)]s	SSSS	(i) quadratic (ii) cubic (iii) arbitrary	1
3-5	4-layered [+/-]s	CFFF SCFF CCSF	(iii) arbitrary	1
3-6	4-layered [+/-]s	SSSS	(i) quadratic (ii) cubic (iii) arbitrary	1.5

Table 3. Convergence of the first four frequencies Ω on the integration rule for the single-layer plate with quadratically shaped fibers (a/b = 1).

No. of division	1st	2nd	3rd	4th
20	48.04	95.11	108.4	162.5
40	47.22	94.18	107.2	161.2
60	46.92	93.83	106.8	160.8
80	46.77	93.65	106.6	160.5
100	46.68	93.54	106.5	160.4
5000	46.34	93.10	106.1	159.8
10000	46.34	93.10	106.1	159.8